Histochemistry and Cell Biology (2026) 164:56
https://doi.org/10.1007/s00418-026-02504-7

RESEARCH

Prenatal 3.5 GHz radiofrequency exposure induces renal histological changes and DNA damage in 6-month-old rats

Elif Gelenli Dolanbay[1] · Fazile Canturk Tan[2] · Hava Bektas[3] · Sumeyye Koc[4] · Salih Varol[2] · Omer Kilic[1] · Unal Uslu[1] · Suleyman Dasdag[5]

Received: 26 February 2026 / Accepted: 3 June 2026
© The Author(s) 2026

Abstract

Early-life environmental stressors may influence long-term organ development and cellular homeostasis. This study investigated whether prenatal exposure to 3.5 GHz radiofrequency radiation (RFR) is associated with renal structural alterations, autophagy-related changes, and DNA damage in adult rat offspring. A total of 24 pregnant Wistar Hannover rats were randomly assigned to sham control, exposure during the last 2 weeks of gestation (D2T: exposure during the last 2 weeks of gestation), or exposure throughout gestation (D3T: exposure throughout gestation) groups ($n = 8$ dams per group). Male offspring were selected and euthanized at 6 months of age. Kidney tissues were examined histopathologically for structural alterations. Autophagy-related markers (Beclin-1 and LC3) were assessed by immunohistochemistry, and DNA damage was evaluated using the comet assay. Statistical analyses were performed using one-way analysis of variance (ANOVA) followed by appropriate post hoc tests. Peak spatial specific absorption rate (psSAR) values in the uterine region were 0.06622 mW/g (1 g averaging) and 0.03825 mW/g (10 g averaging). Prenatal RFR exposure was associated with significant renal histopathological alterations in offspring, most pronounced in the D3T group, including glomerular atrophy, tubular dilation, epithelial vacuolization, and cast formation ($p < 0.01$–0.001 versus controls). Beclin-1 and LC3 expression levels were significantly increased in both exposure groups ($p < 0.001$), suggesting altered autophagy-related marker expression. The comet assay demonstrated significantly increased DNA fragmentation in D2T and D3T groups compared with controls ($p < 0.001$), indicating increased genomic stress. Overall, prenatal exposure to 3.5 GHz RFR is associated with renal structural alterations, increased DNA damage, and changes in autophagy-related markers in adult rat offspring.

Keywords 3.5 GHz · Radiofrequency radiation · Kidney · Autophagy · DNA damage · Rat

✉ Elif Gelenli Dolanbay
elif.dolanbay@medeniyet.edu.tr

Fazile Canturk Tan
fcanturk@erciyes.edu.tr

Hava Bektas
havabektas@yyu.edu.tr

Sumeyye Koc
sumeyyeakin16@gmail.com

Salih Varol
salihvarol@erciyes.edu.tr

Omer Kilic
omerkilicmd@gmail.com

Unal Uslu
unal.uslu@medeniyet.edu.tr

Suleyman Dasdag
sdasdag@gmail.com

[1] Department of Histology and Embryology, Faculty of Medicine, Istanbul Medeniyet University, Unalan Neighborhood, Unalan Street, D-100 Highway Side Road Uskudar, 34700 Istanbul, Turkey

[2] Department of Biophysics, Faculty of Medicine, Erciyes University, Kayseri, Turkey

[3] Department of Biophysics, Faculty of Medicine, Van Yuzuncu Yil University, Van, Turkey

[4] Department of Molecular Biology and Genetics, Bogazici University, Istanbul, Turkey

[5] Department of Biophysics, Faculty of Medicine, İstanbul Medeniyet University, Istanbul, Turkey

Published online: 09 July 2026

Introduction

With the widespread use of wireless communication technologies, concerns regarding the potential health risks of RFR exposure have gained increasing attention. The kidneys, essential organs for maintaining homeostasis, are particularly vulnerable to environmental stressors, including electromagnetic fields (EMFs) (Mahmoudi et al. 2018; Hasan et al. 2021; Zhang et al. 2023). Studies have suggested that prolonged RFR exposure may be associated with cellular stress responses, including processes reported in the literature such as oxidative stress (Oktem et al. 2005; M Fahmy and Mohammed 2015; Berkoz et al. 2018), inflammation (Bodera et al. 2015; Khattab and Marei 2019), and cellular damage in renal tissues (Chauhan et al. 2017; Hasan et al. 2021), potentially contributing to impaired kidney function. However, most existing research has focused on lower-frequency RFR (e.g., 900 MHz, 1800 MHz, and 2.45 GHz Wi-Fi), leaving the biological effects of higher-frequency RFR, such as 3.5 GHz, largely unexplored.

Previous research indicates that RFR exposure has been proposed to be associated with alterations in redox homeostasis, including changes in reactive oxygen species (ROS) levels and antioxidant defense mechanisms, with possible implications for lipid peroxidation, protein oxidation, and mitochondrial function (Ratliff et al. 2016; Dasdag and Akdag 2016). Additionally, chronic RFR exposure has been linked to DNA damage (Verschaeve et al. 2010; Akdag et al. 2018; Bektas et al. 2020; Kaur et al. 2023) and dysregulated autophagic processes (Jangid et al. 2024; Kirimlioglu et al. 2024), both of which are critical for maintaining cellular homeostasis and tissue repair. Despite these findings, the extent to which higher-frequency RFR affects these mechanisms in renal tissues remains unclear.

Emerging evidence suggests that prenatal RFR exposure may pose an even greater risk, as the developing kidney is particularly susceptible to environmental stressors during gestation. Experimental studies indicate that prenatal EMF exposure can lead to structural and functional alterations in renal development (Kilic et al. 2023; Pawar and Martin 2024), including glomerular damage, tubular degeneration, and cellular dysfunction potentially involving processes reported in the literature such as oxidative stress-related pathways (Keles et al. 2025) Potential mechanisms include processes reported in the literature involving reactive oxygen species (ROS),(Bektas et al. 2020, 2021), impaired DNA repair processes (Guler et al. 2010; Vafaei et al. 2020), and disruption of nephrogenesis-regulating signaling pathways (Pyrpasopoulou et al. 2004; Odaci et al. 2015). However, the long-term impact of prenatal exposure to high-frequency RFR remains largely unknown.

Autophagy, a key cellular degradation and recycling process, plays a crucial role in kidney homeostasis under both physiological and pathological conditions (Ma et al. 2022). Its dysregulation has been implicated in various renal disorders, including acute kidney injury, chronic kidney disease, and renal aging (Vafaei et al. 2020). Some studies suggest that RFR exposure interferes with autophagic processes, leading to excessive activation or inhibition of autophagy-related pathways (Bertuccio et al. 2023; Jangid et al. 2024; Kirimlioglu et al. 2024; Kartal et al. 2025). While increased autophagic activity may result in excessive degradation of essential cellular components, insufficient autophagy can cause the accumulation of damaged organelles and toxic aggregates, further contributing to renal dysfunction (Arab et al. 2022; Liang et al. 2022). However, the specific impact of high-frequency RFR on renal autophagy remains largely unexplored.

To address this knowledge gap, our study investigates the effects of prenatal 3.5 GHz RFR exposure on renal tissue, focusing on DNA integrity and autophagy-related markers. We hypothesize that high-frequency RFR exposure may be associated with alterations in key cellular homeostasis mechanisms. Given the vulnerability of the developing kidney to environmental stressors, understanding the long-term consequences of prenatal RFR exposure is important. By comparing our findings with previous research on lower-frequency RFR, this study provides additional insights into the biological effects of high-frequency wireless communication technologies on renal development and function. The study includes 3.5 GHz RF exposure groups during the entire pregnancy and the last 2 weeks of pregnancy, highlighting the effects of RF exposure at different gestational periods.

Materials and methods

Animal models and classification

Ethical approval for this study was obtained from the Animal Experiments Local Ethics Committee of Istanbul Bagcilar Training and Research Hospital (No. 2024/52). A total of 24 pregnant Wistar Hannover rats (with an average gestation period of 21–22 days) were randomly assigned to three experimental groups ($n = 8$ dams per group): sham control, exposure during the last 2 weeks of gestation (D2T), and exposure throughout gestation (D3T).

A total of 24 male offspring were included in the final analyses (Sham control: $n = 8$; D2T: $n = 8$; D3T: $n = 8$). To avoid pseudoreplication and control for litter effects, the litter was considered the experimental unit, and one randomly selected male offspring from each litter was included in all analyses.

To prevent external radiofrequency interference, all groups were housed in separate Faraday cages throughout the exposure period. After birth, offspring were maintained under standardized environmental conditions (temperature: 22 ± 1 °C, relative humidity: 50 ± 10%, 12-h light/dark cycle) until 6 months of age.

At 6 months of age, animals were anesthetized with ketamine (75 mg/kg) and xylazine (10 mg/kg) and euthanized by intracardiac exsanguination. Kidney tissues were harvested for histopathological, immunohistochemical, and molecular analyses.

Exposure and field measurements

A signal generator (model 3500 PM10, Everest Comp., Adapazarı, Turkey) producing a 3.5 GHz radiofrequency waveform was used for exposure standardization. The power output of the signal generator was maintained at 1 W throughout the exposure period. The antenna, designed to mimic a conventional mobile phone antenna, was positioned centrally approximately 50 cm above the exposure cage.

Pregnant rats in the experimental groups were exposed to 3.5 GHz radiofrequency radiation (RFR) for 2 h/day during gestation only. Sham control animals were maintained under identical experimental conditions, except that the signal generator remained switched off. All animals were housed in specially designed Plexiglas cages without metallic components to minimize electromagnetic reflection and distortion. Even the water bottle tips were constructed from Plexiglas tubing to preserve field integrity. Animals were allowed to move freely within the cages.

Each experimental group was housed in a separate Faraday cage throughout irradiation to eliminate environmental electromagnetic interference. The signal generator was positioned outside the Faraday enclosure, whereas the antenna extended inside the cage. A metal reflector was positioned above the antenna to improve field uniformity.

After birth, male offspring were separated and were not exposed to any additional RFR until 6 months of age. Therefore, all observed findings reflected prenatal-only exposure.

Electric field measurements were performed using a calibrated EMR-300 probe (NARDA, Pfullingen, Germany). Field strength was measured at five predefined locations within the exposure cage (four corners and center), yielding values of 24, 26, 26.3, 27, and 28 V/m, respectively, indicating relatively homogeneous electromagnetic field distribution across the exposure area (Gelenli Dolanbay et al. 2025).

Specific absorption rate (SAR) analysis

CST Studio Suite software (CST AG, Darmstadt, Germany) was used to simulate specific absorption rate (SAR) distribution at the rat uterus. The experimental exposure setup was reconstructed in detail to closely replicate the actual irradiation conditions. A high-resolution voxel-based anatomical rat model derived from computed tomography (CT) datasets available in the CST biological model library was used for electromagnetic simulations. The antenna system, reflector, Plexiglas cage structure, and animal positioning were incorporated into the simulation model.

Electromagnetic calculations were performed using the finite integration technique (FIT), enabling simultaneous electromagnetic and thermal simulations. To validate the computational model, simulated electric field values were compared with experimentally measured values obtained using the EMR-300 field probe (NARDA, Pfullingen, Germany). Measurements were obtained from five locations across the exposure plane (four corners and center). No significant variation was observed among measured values, which ranged between 24 and 28 V/m, confirming relatively homogeneous field distribution.

Based on the measured field strengths, peak spatial specific absorption rate (psSAR) values were calculated at 3.5 GHz using CST Studio Suite software and the average measured electric field intensity (Gelenli Dolanbay et al. 2025).

Temperature variations within the exposure environment were continuously monitored using a calibrated type-K thermocouple probe (accuracy ± 0.1 °C) positioned adjacent to the animal exposure area inside the Plexiglas cage. Temperature measurements were recorded at 1-min intervals throughout the entire exposure period using a digital acquisition system. Baseline temperature values were obtained before exposure and continuously compared with measurements recorded during RFR exposure.

No statistically or biologically significant temperature increase was detected during 3.5 GHz exposure at 1 W output power. The maximum observed temperature variation remained within ± 0.2 °C of baseline values, which is within the physiological fluctuation range for laboratory rodents.

All metallic materials were excluded from the exposure environment to minimize electromagnetic reflection artifacts. Thermal effects were additionally considered during SAR simulations; however, neither computational nor experimental analyses demonstrated evidence of thermal overload conditions (Gelenli Dolanbay et al. 2025).

Tissue processing and immunohistochemical analysis

Kidney tissue specimens fixed in 10% neutral buffered formalin (NBF) were routinely processed, embedded in paraffin blocks, and sectioned at 5 µm thickness for hematoxylin–eosin (H&E) staining. Sections prepared for immunohistochemistry (IHC) were deparaffinized in xylene and rehydrated through graded ethanol series followed by

distilled water for 5 min. Subsequently, sections were rinsed with TBS-T buffer (480 mL distilled water, 20 mL Tris-buffered saline [TBS], and 500 µL Tween-20) and incubated for 15 min at 37 °C in 0.1% Triton X-100 prepared in phosphate-buffered saline (PBS). Antigen retrieval was performed using heat-induced epitope retrieval in citrate buffer (pH 6.0) with microwave treatment at 800 W until boiling, followed by 2-min cooling intervals, repeated five times (Magaki et al. 2019).

Histological examination and evaluation

Histological evaluation was performed under light microscopy (Olympus BX53). Histopathological alterations, including glomerular atrophy, vacuolization (Vac), tubular dilation (TubDil), hemorrhage, and cast formation (Cast), were assessed among the groups (Okatan et al. 2018).

The immunohistochemical (IH) score was determined using a semiquantitative approach, as previously described by Kanbe et al. (2014). The quantification of staining intensity was achieved using a visual analogue scale (VAS) ranging from 0 to 100 mm. The scoring system was categorized into six grades based on the percentage of positive staining: The following gradings are employed: grade 0 (0%), grade 1 (< 5%), grade 2 (5–20%), grade 3 (20–40%), grade 4 (40–60%), and grade 5 (60–100%). The cumulative IH grades obtained from four different microscopic fields were summed to generate the final IH score for each renal specimen. For instance, a total IH score of 11 was yielded by scores of 2, 3, 1, and 5 obtained from four different microscopic fields.

Histological and immunohistochemical evaluations were performed independently by investigators blinded to the experimental groups to minimize observer bias.

Autophagic activity (immunohistochemistry)

Immunohistochemical staining for Beclin-1 and LC3 was performed to assess autophagy-related protein expression in renal tissue. Following antigen retrieval and blocking procedures, tissue sections were incubated overnight at 4 °C with primary antibodies against Beclin-1 (Lot no: 230103481; Epitomics, Burlingame, CA, USA; dilution 1:200) and LC3 (Lot no: orb33328; Biorbyt, Cambridge, UK; dilution 1:200). On the following day, sections were incubated with horseradish peroxidase (HRP)-conjugated secondary antibodies, and immunoreactivity was visualized using 3,3′-diaminobenzidine (DAB) chromogen (Maroni et al. 2024). Sections were counterstained with hematoxylin and mounted with synthetic mounting medium.

Negative control sections were processed simultaneously by omitting the primary antibody to confirm staining specificity. Antibody specificity was additionally supported by manufacturer validation data and previous studies demonstrating the use of these antibodies in renal tissue. The observed staining pattern was consistent with the expected cytoplasmic localization reported in the literature.

To evaluate interobserver reliability, two independent blinded observers analyzed 24 samples representing different IH score stages for Beclin-1 and LC3 on two separate occasions.

As immunohistochemistry alone does not directly assess autophagic flux, the findings were interpreted as changes in autophagy-related protein expression rather than definitive evidence of altered autophagic activity or impaired autophagic flux.

DNA damage (comet assay)

DNA damage in kidney tissue was assessed using the neutral comet assay. Briefly, a 0.5 g kidney tissue sample was excised, minced, and suspended in 2 mL cold PBS. The mixture was agitated at 500 rpm for 5 min and subsequently incubated on ice for 10 min. The resulting supernatant was used for comet assay slide preparation according to a standardized protocol (Baran et al. 2022).

Slides were examined using an Olympus BX51 fluorescence microscope (Tokyo, Japan) at 200× magnification. One slide was prepared for each animal, resulting in a total of 24 slides. A total of 50 randomly selected cells from each animal were analyzed using the Comet Assay Software Project (CASP v1.2.2; Windows 2010), an automated image analysis system.

DNA damage parameters including head length, tail length, comet length, head DNA (%), tail DNA (%), tail moment, and olive tail moment were quantified. Cells exhibiting comet-like tail formation were classified as DNA-damaged, whereas nuclei without detectable tails were considered undamaged (Yalcin et al. 2023).

All comet assay analyses were performed in a blinded manner to ensure objective evaluation and reproducibility.

Statistical analysis

Statistical analyses were performed using SPSS software (Version 20.0; IBM SPSS Inc., Chicago, IL, USA). Data are presented as mean ± standard deviation (SD). The normality of distribution for OTM, TM, TAIL DNA, HEAD DNA, L. COMET, L. TAIL, and L. HEAD variables was assessed using the Kolmogorov–Smirnov test. For variables that did not show a normal distribution (OTM, TM, TAIL DNA, HEAD DNA, L. COMET, and L. TAIL), the Kruskal–Wallis test was applied to compare differences among groups. When significant differences were detected, post hoc pairwise comparisons were performed using the Conover test (Conover 1980). For normally distributed data (L. HEAD),

one-way analysis of variance (ANOVA) was used to evaluate group differences, followed by Duncan's multiple range test for post hoc comparisons. Duncan's test was selected owing to its suitability for identifying intergroup differences in balanced experimental designs with equal sample sizes.

All statistical tests were two-tailed, and exact *p*-values were reported where applicable. Statistical significance was defined as $p < 0.05$.

Results

The peak spatial specific absorption rate (psSAR), calculated in accordance with IEEE/IEC 62704-1 standards, was 0.06622 mW/g for 1 g tissue and 0.03825 mW/g for 10 g tissue, indicating low-level prenatal exposure under the experimental conditions.

Histopathological evaluation of renal tissues demonstrated significant intergroup differences in glomerular atrophy, tubular vacuolization, tubular dilatation, cast formation, Beclin-1 expression, and LC3 expression (Table 1, Fig. 1). Hemorrhage did not differ significantly among groups ($p = 0.41$).

Glomerular atrophy was significantly increased in the D3T group compared with both the sham control and D2T groups ($p = 0.0021$), indicating a gestation-duration–dependent effect of prenatal RFR exposure (Fig. 1c).

Tubular vacuolization showed a significant increase in the D3T group compared with both the sham control and D2T groups ($p = 0.0026$), whereas the D2T group showed intermediate values relative to controls (Fig. 1d–f).

Tubular dilatation was significantly elevated in both exposure groups compared with the sham control group, with the highest levels observed in the D3T group ($p = 1.42 \times 10^{-17}$) (Fig. 1g–i).

Cast formation showed a significant intergroup difference ($p = 0.0155$), with higher values observed in the D3T group compared with the other groups (Fig. 1m–o).

Beclin-1 expression was significantly increased in both D2T and D3T groups compared with sham control ($p = 2.22 \times 10^{-4}$), with maximal expression in the D3T group (Fig. 2a–c).

Similarly, LC3 expression was significantly elevated in both exposure groups compared with controls ($p = 2.54 \times 10^{-9}$), again showing the highest levels in the D3T group (Fig. 2d–f).

DNA damage analysis demonstrated significant intergroup differences across all comet assay parameters, including head length, tail length, total comet length, head DNA percentage, tail DNA percentage, tail moment (TM), and olive tail moment (OTM) (Table 2, Fig. 3; all *p* values as reported in Table 2).

Both D2T and D3T groups showed significant increases in DNA damage indices compared with the sham control group (all $p < 0.001$ in Table 2), with more pronounced alterations in the D3T group, indicating a duration-dependent genotoxic effect of prenatal 3.5 GHz RFR exposure.

Discussion

The increasing deployment of wireless communication systems operating in the 3.5 GHz frequency range has raised ongoing scientific interest regarding potential biological effects of radiofrequency radiation (RFR), particularly during early developmental periods. In the present experimental study, prenatal exposure to 3.5 GHz RFR was associated with structural and molecular alterations in rat kidney tissue at 6 months of age, including histological changes, increased DNA damage indices, and modulation of autophagy-related protein expression. While these findings do not establish causality in humans, they contribute to the expanding experimental literature evaluating frequency-specific biological responses to RFR exposure.

Histological evaluation demonstrated glomerular atrophy, tubular dilation, vacuolization, and cast formation in RFR-exposed groups, with more pronounced changes in the D3T

Table 1 Differences in histopathological parameters between groups

Group	n	Atrophy ($x \pm Sx$)	Vac ($x \pm Sx$)	TubDil ($x \pm Sx$)	Hemorrhage ($x \pm Sx$)	Cast ($x \pm Sx$)	Beclin-1 ($x \pm Sx$)	LC3 ($x \pm Sx$)
Sham control	8	2.38 ± 0.32^{b}	1.88 ± 0.52^{b}	2.09 ± 0.23^{b}	3.75 ± 0.75	0.63 ± 0.32^{bc}	2.91 ± 0.21^{b}	2.63 ± 0.19^{b}
D2T	8	4.50 ± 0.85^{b}	1.50 ± 0.38^{b}	4.59 ± 0.19^{a}	5.50 ± 0.76	0.50 ± 0.19^{c}	3.84 ± 0.19^{a}	4.03 ± 0.17^{a}
D3T	8	6.88 ± 0.91^{a}	4.00 ± 0.50^{a}	5.63 ± 0.27^{a}	5.50 ± 1.20	1.63 ± 0.38^{ab}	4.00 ± 0.19^{a}	4.19 ± 0.15^{a}
p		**	**	***	NS	*	***	***
p value		**0.0021**	**0.0026**	**1.42×10^{-17}**	**0.41**	**0.0155**	**2.22×10^{-4}**	**2.54×10^{-9}**

a,b,c Different superscript letters indicate significant differences between groups, Vac tubular vacuolization, *TubDil* tubular dilatation, *Cast* cast formation. *$p < 0{,}05$, **$p < 0{,}01$, ***$p < 0{,}001$, *NS* not significant. *x* mean, *Sx* SEM

Bold values indicate statistically significant differences compared with the sham group

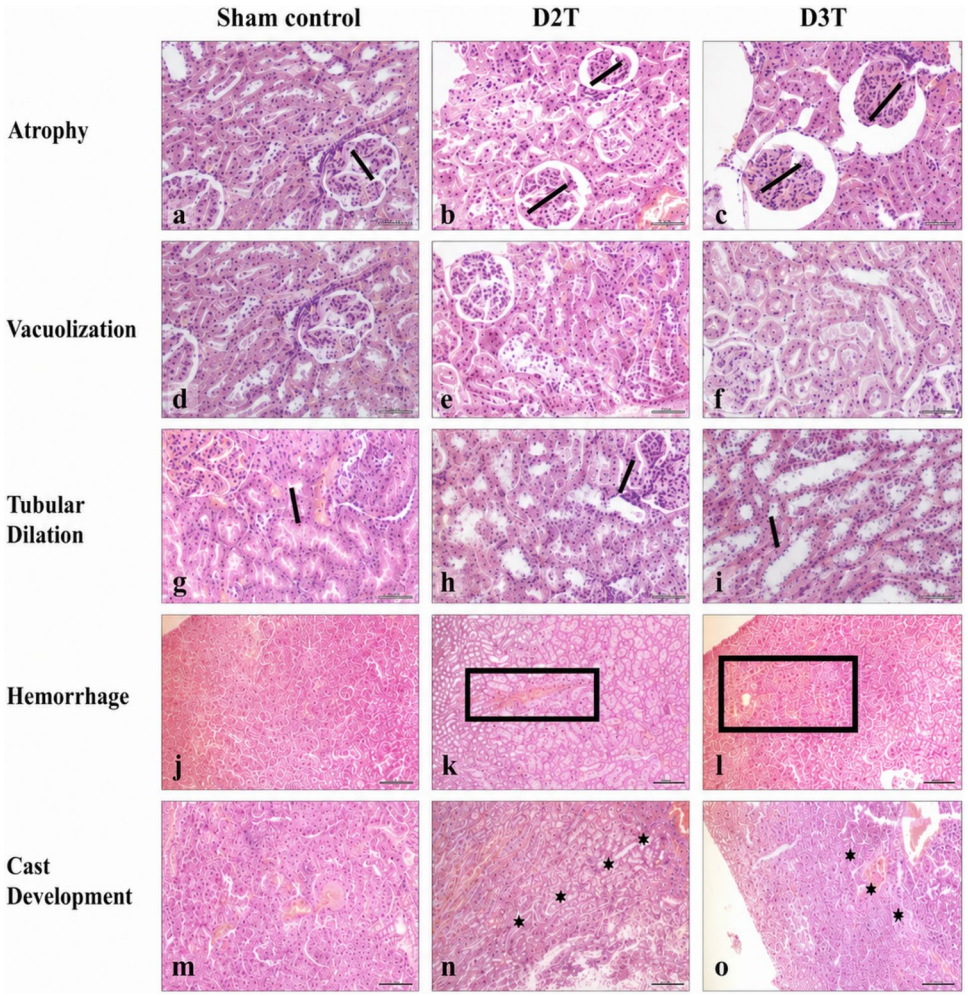


Fig. 1 Hematoxylin and eosin (H&E)-stained sections of kidney tissue from radiofrequency radiation (RFR)-exposed rats. Panels **a**, **d**, **g**, **j**, and **m** represent the sham conrol group. Panels **b** and **c** show tubular atrophy; panels **e** and **f** demonstrate cytoplasmic vacuolization; panels **h** and **i** illustrate tubular dilatation; panels **k** and **l** indicate hemorrhage; and panels **n** and **o** reveal cast formation in the D2T and D3T exposure groups, respectively. Scale bar = 50 µm

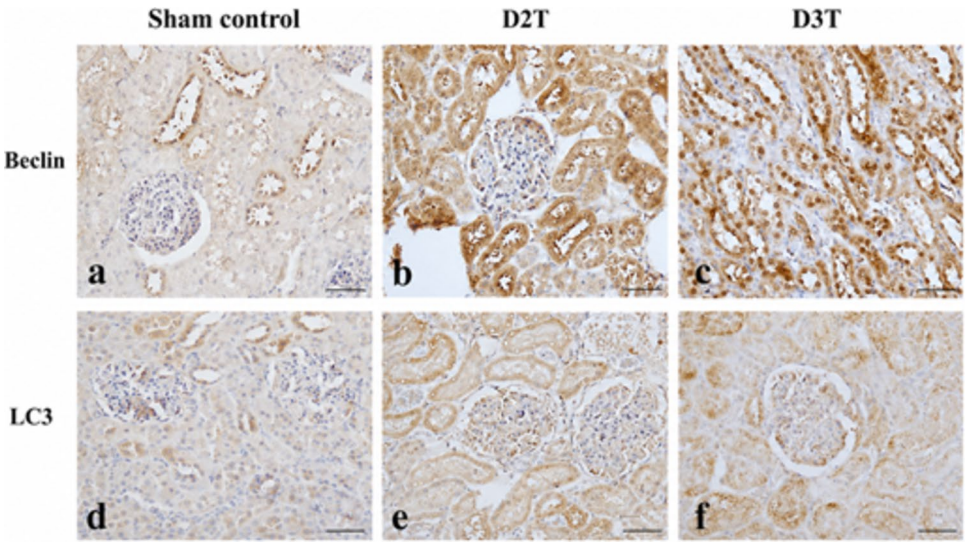


Fig. 2 Immunohistochemical staining of kidney tissue from radiofrequency radiation (RFR)-exposed rats. Panels **a** and **d** represent the sham control group. Panels **b** and **c** show increased Beclin-1 expression, whereas panels **e** and **f** demonstrate elevated LC3 expression in the D2T and D3T groups, respectively. Positive immunoreactivity was observed predominantly in proximal tubular epithelial cells. Scale bar = 200 µm for panel d; 50 µm for panels a, b, c, e, and f

group. These findings are consistent with previous experimental reports at lower frequencies (900 MHz–2.45 GHz), suggesting that renal tissue may exhibit sensitivity to RF-related stress across different exposure ranges (Oktem et al. 2005; Ozorak et al. 2013; Ulubay et al. 2015). The graded morphological alterations observed between

Table 2 Differences in DNA damage parameters between groups

Group	*n*	L.Head ($x \pm Sx$)	L.Tail ($x \pm Sx$)	L.Comet ($x \pm Sx$)	Head DNA ($x \pm Sx$)	Tail DNA ($x \pm Sx$)	TM ($x \pm Sx$)	OTM ($x \pm Sx$)
Sham control	8	129 ± 2.76^{c}	24.8 ± 1.34^{b}	153.8 ± 3.62^{b}	95.94 ± 0.13^{a}	4.06 ± 0.13^{c}	1.22 ± 0.06^{c}	2.16 ± 0.12^{c}
D2T	8	227.24 ± 5.96^{a}	175.02 ± 6.54^{a}	408.02 ± 9.42^{a}	80.08 ± 0.65^{b}	19.92 ± 0.65^{b}	35.96 ± 2.23^{b}	29.08 ± 1.34^{b}
D3T	8	208.24 ± 4.13^{b}	172.1 ± 6.93^{a}	377.44 ± 9.48^{a}	74.26 ± 0.27^{c}	25.74 ± 0.27^{a}	44.52 ± 2.06^{a}	33.54 ± 0.96^{a}
p		***	***	***	***	***	***	***
p-value		3.3725×10^{-17}	7.9384×10^{-4}	1.3605×10^{-22}	2.0441×10^{-17}	1.1686×10^{-17}	1.2233×10^{-10}	4.2037×10^{-12}

a,b,c Different superscript letters indicate significant differences between groups. *L.* length, *TM* tail moment, *OTM* olive tail moment. ***$p < 0{,}001$, *x* mean, *Sx* SEM

Bold values indicate statistically significant differences compared with the sham group

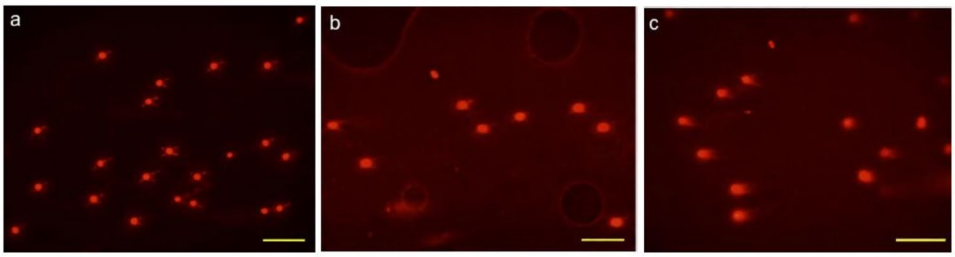


Fig. 3 Representative images of the neutral comet assay performed in kidney cells. Panel **a**: sham control group (Tail DNA: 4.06%); panel **b**: D2T group (Tail DNA: 19.92%); panel **c**: D3T group (Tail DNA: 25.74%). Ethidium bromide staining, original magnification × 200. Scale bar = 200 µm

exposure groups may indicate a relationship between duration of prenatal exposure and tissue susceptibility. However, differences in experimental design and dosimetry across studies limit direct comparisons.

In the present study, increased Beclin-1 and LC3 immunoreactivity was observed in renal tissue following prenatal RFR exposure. These proteins are widely used markers associated with autophagy-related pathways. However, since autophagic flux was not directly assessed, these findings should be interpreted as changes in autophagy-related protein expression rather than definitive evidence of altered autophagic activity. This interpretation is consistent with previous studies reporting variable autophagy responses following RF exposure, depending on frequency, exposure duration, and tissue-specific factors (Kim et al. 2016; Sannino et al. 2022; Golbach et al. 2015).

Comet assay analysis demonstrated significant increases in DNA fragmentation parameters in RFR-exposed groups, indicating increased genomic stress in renal tissue. These findings are in agreement with previous experimental studies reporting DNA damage and strand breaks following RF exposure, which have been discussed in the literature in the context of oxidative stress-related processes (Dasdag and Akdag 2016; Alkis et al. 2019). Nevertheless, inconsistencies in the literature suggest that genotoxic outcomes may be highly dependent on exposure conditions, biological context, and methodological differences.

The developing kidney appears to be particularly sensitive to environmental stressors, including prenatal RF exposure. Experimental developmental studies have reported structural renal alterations following embryonic exposure, including tubular and glomerular abnormalities (Rehman 2015; Dsilva et al. 2022). These findings, together with maternal exposure models, suggest that prenatal life may represent a critical window of susceptibility for renal tissue development (Raouf and Girgis 2022; Celegen et al. 2024).

Epidemiological and experimental studies have suggested that prolonged RFR exposure may be associated with cellular stress responses, including processes reported in the literature such as oxidative stress, inflammation, and cellular damage in renal tissues (Zhang et al. 2023; Mahmoudi et al. 2018; Hasan et al. 2021). Therefore, extrapolation of experimental findings to clinical outcomes should be made cautiously.

Several limitations should be acknowledged. Only male offspring were included, which limits sex-based interpretation. In addition, a single frequency (3.5 GHz) and exposure protocol were used, limiting generalizability across different RF conditions. Furthermore, mechanistic interpretation is based on marker expression and DNA damage

assessment rather than functional pathway analysis or interventional validation.

Future studies should incorporate oxidative stress biomarkers, autophagic flux measurements, and senescence-related end points to better elucidate underlying mechanisms. Comparative studies across different frequencies and exposure intensities would also help clarify dose–response relationships and biological thresholds.

Prenatal exposure to 3.5 GHz RFR was associated with renal histological alterations, increased DNA damage indices, and changes in autophagy-related protein expression in adult rat offspring. These findings extend previous experimental observations at lower frequencies and suggest that the developing kidney may exhibit increased susceptibility to prenatal RF exposure under controlled experimental conditions. However, given the limitations of the study design, these results should be interpreted as experimental evidence of biological association rather than causal evidence of disease or functional impairment in humans.

Acknowledgements We sincerely thank Prof. Claudio Enrique Fernández Rodríguez, Prof. Mehmet Faruk Oktay for their valuable contributions and support to our study. The authors are also grateful to Kerem Dolanbay for his consistent support throughout the study.

Author contributions EGD and SD conceived and designed the study. EGD performed the histological examinations and contributed significantly to the experimental design. EGD, FCT, HB, SK, OK, UU, SV, and SD performed the experiments and contributed to sample collection and laboratory analyses. EGD and SD performed the data analysis and interpretation. All authors contributed to the interpretation of the data, critically revised the manuscript for important intellectual content, and approved the final version for submission.

Funding Open access funding provided by the Scientific and Technological Research Council of Türkiye (TÜBİTAK). Open access funding provided by the Scientific and Technological Research Council of Türkiye (TÜBİTAK). The authors received no specific funding for this research other than the aforementioned open access support.

Data availability The data that supports the findings of this study are available from the corresponding author upon reasonable request.

Declarations

Conflict of interest The authors declare no competing interests.

Ethical approval Ethical approval for this research was obtained from the Animal Experiments Local Ethics Committee at Istanbul Bagcilar Training and Research Hospital (No. 2024/52).

Human and animal rights All animal procedures were conducted in accordance with the guidelines of the 'Principles of Laboratory Animal Care' (NIH Publication Vol 25, No. 28 revised 1996; http://grants.nih.gov/grants/guide/notice-files/not96-208.html).

Use of generative AI assisted tools The manuscript was reviewed for language clarity and readability using AI-assisted language editing tools. The authors take full responsibility for the content of the manuscript.

Open Access This article is licensed under a Creative Commons Attribution 4.0 International License, which permits use, sharing, adaptation, distribution and reproduction in any medium or format, as long as you give appropriate credit to the original author(s) and the source, provide a link to the Creative Commons licence, and indicate if changes were made. The images or other third party material in this article are included in the article's Creative Commons licence, unless indicated otherwise in a credit line to the material. If material is not included in the article's Creative Commons licence and your intended use is not permitted by statutory regulation or exceeds the permitted use, you will need to obtain permission directly from the copyright holder. To view a copy of this licence, visit http://creativecommons.org/licenses/by/4.0/.

References

Akdag M, Dasdag S, Canturk F, Akdag MZ (2018) Exposure to non-ionizing electromagnetic fields emitted from mobile phones induced DNA damage in human ear canal hair follicle cells. Electromagn Biol Med 37(2):66–75. https://doi.org/10.1080/15368378.2018.1463246

Alkis ME, Bilgin HM, Akpolat V, Dasdag S, Yegin K, Yavas MC, Akdag MZ (2019) Effect of 900-, 1800-, and 2100-MHz radiofrequency radiation on DNA and oxidative stress in brain. Electromagn Biol Med 38(1):32–47. https://doi.org/10.1080/15368378.2019.1567526

Arab HH, Abd El-Aal SA, Eid AH, Arafa ESA, Mahmoud AM, Ashour AM (2022) Targeting inflammation, autophagy, and apoptosis by troxerutin attenuates methotrexate-induced renal injury in rats. Int Immunopharmacol 103:108284. https://doi.org/10.1016/j.intimp.2021.108284

Baran M, Yay A, Onder GO, Canturk Tan F, Yalcin B, Balcioglu E, Yildiz OG (2022) Hepatotoxicity and renal toxicity induced by radiation and the protective effect of quercetin in male albino rats. Int J Radiat Biol 98(9):1473–1483. https://doi.org/10.1080/09553002.2022.2033339

Bektas H, Dasdag S, Bektas MS (2020) Comparison of effects of 2.4 GHz Wi-Fi and mobile phone exposure on human placenta and cord blood. Biotechnol Biotechnol Equip 34(1):154–162. https://doi.org/10.1080/13102818.2020.1725639

Bektas H, Dasdag S, Bektas MS (2021) Evaluation of 900 and 1800 MHz radiofrequency radiation emitted from mobile phones on pregnant women. J Int Dent Med Res 14(4):1633–1639

Berkoz M, Arslan B, Yildirim M, Aras N, Yalin S, Comelekoglu U (2018) 1800 MHz radio-frequency electromagnetic radiation induces oxidative stress in rat liver, kidney and brain tissues. Eastern J Med 23(2):71–78. https://doi.org/10.5505/ejm.2018.20982

Bertuccio MP, Acri G, Ientile R, Caccamo D, Curro M (2023) Exposure to 2.45 GHz electromagnetic radiation induced different cell responses in neuron-like cells and peripheral blood mononuclear cells. Biomedicines. 11(12):3129. https://doi.org/10.3390/biomedicines11123129

Bodera P, Stankiewicz W, Antkowiak B, Paluch M, Kieliszek J, Sobiech J, Niemcewicz M (2015) Influence of electromagnetic field (1800 MHz) on lipid peroxidation in brain, blood, liver and kidney in rats. Int J Occup Med Environ Health 28(4):751–759. https://doi.org/10.13075/ijomeh.1896.00255

Celegen K, Ozgul E, Yesildag Z, Camirci EY, Celegen M, Bukulmez A. 2024. Risk factors of congenital anomalies of the kidney and urinary tract (CAKUT): Exposure to mobile phones during

pregnancy. *Turk J Med Sci.* 54(1):291–300. https://doi.org/10.55730/1300-0144.5790

Chauhan P, Verma HN, Sisodia R, Kesari KK (2017) Microwave radiation (2.45 GHz)-induced oxidative stress: whole-body exposure effect on histopathology of Wistar rats. Electromagn Biol Med 36(1):20–30. https://doi.org/10.3109/15368378.2016.1144063

Conover WJ (1980) Practical nonparametric statistics, 2nd edn. Wiley, New York (NY), p 493

Dasdag S, Akdag MZ (2016) The link between radiofrequencies emitted from wireless technologies and oxidative stress. J Chem Neuroanat 75(Pt B):85–93. https://doi.org/10.1016/j.jchemneu.2015.09.001

Dsilva MH, Swer RT, Anbalagan J (2022) Histomorphometric analysis of chick embryo kidneys on exposure to 1800 MHz and 2100 MHz radiofrequency radiation emitted from cell phone. J Clin Diagn Res 16(3):1–6. https://doi.org/10.7860/JCDR/2022/58391.16862

Fahmy HM, Mohammed FF (2015) Effect of radiofrequency waves emitted from conventional Wi-Fi devices on some oxidative stress parameters in rat kidney. J Drug Metab Toxicol. 6(5):1–6. https://doi.org/10.4172/2157-7609.1000195

Gelenli Dolanbay E, Mert T, Caliskan Bender G, Bektas H, Uslu U, Fernandez-Rodriguez CE, Dasdag S (2025) Male reproductive and cellular damage after prenatal 3.5 GHz radiation exposure: one-year postnatal effects. Ann New York Acad Sci. 1554(1):140–152. https://doi.org/10.1111/nyas.70116

Golbach LA, Scheer MH, Cuppen JJM, Savelkoul H, Verburg-Van Kemenade BML (2015) Low-frequency electromagnetic field exposure enhances extracellular trap formation by human neutrophils through the NADPH pathway. J Innate Immun 7(5):459–465. https://doi.org/10.1159/000380764

Guler G, Tomruk A, Ozgur E, Seyhan N (2010) The effect of radiofrequency radiation on DNA and lipid damage in non-pregnant and pregnant rabbits and their newborns. Gen Physiol Biophys 29(1):59–66. https://doi.org/10.4149/gpb_2010_01_59

Hasan I, Amin T, Alam MR, Islam MR (2021) Hematobiochemical and histopathological alterations of kidney and testis due to exposure of 4G cell phone radiation in mice. Saudi J Biol Sci 28(5):2933–2942. https://doi.org/10.1016/j.sjbs.2021.02.028

Jangid P, Rai U, Singh R (2024) Radio frequency electromagnetic radiations interfere with the Leydig cell functions in vitro. PLoS ONE 19(5):e0299017. https://doi.org/10.1371/journal.pone.0299017

Kanbe K, Hara R, Chiba J, Inoue Y, Taguchi M, Tanaka Y (2014) Application of a new immunohistology scoring system (IH score): Analysis of TNF-α in synovium related to disease activity score in infliximab-treated patients with rheumatoid arthritis. Mod Rheumatol 24(6):910–914. https://doi.org/10.3109/14397595.2014.887047

Kartal B, Alimogullari E, Akkurt G, Alimogullari M, Cayli S (2025) The histological investigation of the effects of electromagnetic radiation on rat ovaries. J Mol Histol 56(1):1–12. https://doi.org/10.1007/s10735-024-10319-w

Kaur P, Rai U, Singh R (2023) Genotoxic risks to male reproductive health from radiofrequency radiation. Cells 12(4):5954. https://doi.org/10.3390/cells12040594

Keles AI, Kaya H, Keles G, Erol HS, Mercantepe T, Odaci E (2025) Exposure to a 0.9-GHz electromagnetic field on postnatal days 21–45 may trigger the renin–angiotensin system in male rat: a histological and biochemical study. J Mol Histol. 56(1):1–13. https://doi.org/10.1007/s10735-024-10317-y

Khattab NF, Marei ES (2019) The role of ferulic acid in the amelioration of kidney changes of rats exposed to electromagnetic radiation. Int J Radiat Res. 17(1):75–85. https://doi.org/10.18869/acadpub.ijrr.17.1.75

Kilic A, Ustunova S, Bulut H, Meral I (2023) Pre- and postnatal exposure to 900 MHz electromagnetic fields induce inflammation and oxidative stress, and alter renin-angiotensin system components differently in male and female offspring. Life Sci 321:121627. https://doi.org/10.1016/j.lfs.2023.121627

Kim JH, Huh YH, Kim HR (2016) Induction of autophagy in the striatum and hypothalamus of mice after 835 MHz radiofrequency exposure. PLoS ONE 11(4):e0153308. https://doi.org/10.1371/journal.pone.0153308

Kirimlioglu E, Oflamaz AO, Hidisoglu E, Ozen S, Yargicoglu P, Demir N (2024) Short and long-term 2100 MHz radiofrequency radiation causes endoplasmic reticulum stress in rat testis. Histochem Cell Biol 162(4):311–321. https://doi.org/10.1007/s00418-024-02308-7

Liang S, Wu YS, Li DY, Tang JX, Liu HF (2022) Autophagy and renal fibrosis. Aging Dis 13(3):712–731. https://doi.org/10.14336/ad.2021.1027

Ma Y, Su Q, Yue C, Zou H, Zhu J, Zhao H, Song R, Liu Z (2022) The effect of oxidative stress-induced autophagy by cadmium exposure in kidney, liver, and bone damage, and neurotoxicity. Int J Mol Sci 23(21):13491. https://doi.org/10.3390/ijms232113491

Magaki S, Hojat SA, Wei B, So A, Yong WH (2019) An introduction to the performance of immunohistochemistry. Methods Mol Biol 1897:289–302. https://doi.org/10.1007/978-1-4939-8935-5_25

Mahmoudi G, Nikzad S, Mehrpouyan M, Moslehi M, Baradaran-Ghahfarokhi M, Dashty A (2018) Effects of mobile phone prolonged radiation on kidney cells; an in-vitro study. J Renal Inj Prev. 7(3):175–179. https://doi.org/10.15171/jrip.2018.42

Maroni P, Lombardi G, Ferraretto A, Bendinelli P (2024) Immunohistochemistry analysis of autophagy-related proteins Beclin-1, p62/SQSTM1, and LC3B in breast carcinoma progression to bone metastasis. Pathol Res Pract 260:155414. https://doi.org/10.1016/j.prp.2024.155414

Odaci E, Unal D, Mercantepe T, Topal Z, Hanci H, Turedi S, Erol HS, Mungan S, Kay H, Colakoglu S (2015) Pathological effects of prenatal exposure to a 900 MHz electromagnetic field on the 21-day-old male rat kidney. Biotech Histochem 90(2):93–101. https://doi.org/10.3109/10520295.2014.947322

Okatan DO, Okatan AE, Hanci H, Demir S, Yaman SO, Colakoglu S, Odaci E (2018) Effects of 900-MHz electromagnetic fields exposure throughout middle/late adolescence on the kidney morphology and biochemistry of the female rat. J Toxicol Environ Health 34(10):693–702. https://doi.org/10.1177/0748233718781292

Oktem F, Ozguner F, Mollaoglu H, Koyu A, Uz E (2005) Oxidative damage in the kidney induced by 900-MHz-emitted mobile phone: protection by melatonin. Arch Med Res 36(4):350–355. https://doi.org/10.1016/j.arcmed.2005.03.021

Ozorak A, Naziroglu M, Celik O, Yuksel M, Ozcelik D, Ozkaya MO, Cetin H, Kahya MC, Kose SA (2013) Wi-Fi (2.45 GHz)- and mobile phone (900 and 1800 MHz)-induced risks on oxidative stress and elements in kidney and testis of rats during pregnancy and development of offspring. Biol Trace Elem Res. 156(1–3):221–229. https://doi.org/10.1007/s12011-013-9836-z

Pawar MG, Martin RE (2024) Effects of exposure to electromagnetic fields (EMFs) on biological systems. Asian J Biol 20(6):21–33. https://doi.org/10.9734/ajob/2024/v20i6412

Pyrpasopoulou A, Kotoula V, Cheva A, Hytiroglou P, Nikolakaki E, Magras IN, Xenos TD, Tsiboukis TD, Karkavelas G (2004) Bone morphogenetic protein expression in newborn rat kidneys after prenatal exposure to radiofrequency radiation. Bioelectromagnetics 25(3):216–227. https://doi.org/10.1002/bem.10185

Raouf AAE, Girgis SM (2022) The effect of electromagnetic waves of mobile phones on DNA, RNA content and kidney function in rats before, during and after pregnancy and their offspring. GSC Adv Res Rev. 13(1):85–91. https://doi.org/10.30574/gscarr.2022.13.1.0264

Ratliff BB, Abdulmahdi W, Pawar R, Wolin MS (2016) Oxidant mechanisms in renal injury and disease. Antioxid Redox Signal 25(3):119–146. https://doi.org/10.1089/ars.2016.6665

Rehman S, Wahab N, Khan H, Qureshi AR (2015) Effects of cell phone radiations on the metanephros tubules in a chick embryo model. J Islamic Int Med Coll 10(4):275–279

Sannino A, Scarfi MR, Dufossée M, Romeo S, Poeta L, Prouzet-Mauleon V, Priault M, Zeni O (2022) Inhibition of autophagy negates radiofrequency-induced adaptive response in SH-SY5Y neuroblastoma cells. Int J Mol Sci 23(15):8414. https://doi.org/10.3390/ijms23158414/s1

Ulubay M, Yahyazadeh A, Deniz G, Kivrak EG, Altunkaynak BZ, Erdem G, Kaplan S (2015) Effects of prenatal 900 MHz electromagnetic field exposures on the histology of rat kidney. Int J Radiat Biol 91(1):35–41. https://doi.org/10.3109/09553002.2014.950436

Vafaei H, Kavari G, Izadi HR, Dorahi ZZ, Dianatpour M, Daneshparvar A, Jamhiri I (2020) Wi-Fi (2.4 GHz) affects antioxidant capacity, DNA repair genes expression, and apoptosis in pregnant mouse placenta. Iran J Basic Med Sci. 23(6):833–842. https://doi.org/10.22038/ijbms.2020.40184.9512

Verschaeve L, Juutilainen J, Lagroye I, Miyakoshi J, Saunders R, de Seze R, Tenforde T, van Rongen E, Veyret B, Xu Z (2010) In vitro and in vivo genotoxicity of radiofrequency fields. Mutat Res 705(3):252–268. https://doi.org/10.1016/j.mrrev.2010.10.001

Yalcin B, Yay AH, Cantürk Tan F, Özdamar S, Yildiz OG (2023) Investigation of the anti-oxidative and anti-inflammatory effects of melatonin on experimental liver damage by radiation. Pathol Res Pract 246:154477. https://doi.org/10.1016/j.prp.2023.154477

Zhang Y, Zhang Y, Ye Z, Yang S, Liu M, Wu Q, Zhou C, He P, Qin X (2023) Mobile phone use, genetic susceptibility and new-onset chronic kidney diseases. Int J Public Health 68:1605358. https://doi.org/10.3389/ijph.2023.1605358

Publisher's Note Springer Nature remains neutral with regard to jurisdictional claims in published maps and institutional affiliations.